



## RESEARCH LETTER

10.1002/2013GL058780

## Key Points:

- Shipborne lidar observations along the Saharan Air Layer from 60°W to 20°W
- Comparing shipborne lidar measurements and results from the model COSMO-MUSCAT
- Properties of the Saharan Air Layer after a travel distance of >10 and 2 days

## Correspondence to:

T. Kanitz,  
kanitz@tropos.de

## Citation:

Kanitz, T., R. Engelmann, B. Heinold, H. Baars, A. Skupin, and A. Ansmann (2014), Tracking the Saharan Air Layer with shipborne lidar across the tropical Atlantic, *Geophys. Res. Lett.*, 41, 1044–1050, doi:10.1002/2013GL058780.

Received 21 NOV 2013

Accepted 6 JAN 2014

Accepted article online 8 JAN 2014

Published online 5 FEB 2014

This is an open access article under the terms of the Creative Commons Attribution-NonCommercial-NoDerivs License, which permits use and distribution in any medium, provided the original work is properly cited, the use is non-commercial and no modifications or adaptations are made.

## Tracking the Saharan Air Layer with shipborne lidar across the tropical Atlantic

T. Kanitz<sup>1</sup>, R. Engelmann<sup>1</sup>, B. Heinold<sup>1</sup>, H. Baars<sup>1</sup>, A. Skupin<sup>1</sup>, and A. Ansmann<sup>1</sup><sup>1</sup>Leibniz Institute for Tropospheric Research, Leipzig, Germany

**Abstract** Saharan dust was observed with shipborne lidar from 60° to 20°W along 14.5°N during a 1-month transatlantic cruise of the research vessel *Meteor*. About 4500 km off the coast of Africa, mean extinction and backscatter-related Ångström exponent of 0.1, wavelength-independent extinction-to-backscatter ratios (lidar ratios) of around 45 sr, and particle linear depolarization ratio of 20% were found for aged dust (transport time >10 days). In contrast, dust with a shorter atmospheric residence time of 2–3 days showed Ångström exponents of –0.5 (backscatter coefficient) and 0.1 (extinction coefficient), mean lidar ratios of 64 and 50 sr, and particle linear depolarization ratios of 22 and 26% at 355 and 532 nm wavelength, respectively. Traces of fire smoke were also detected in the observed dust layers. The lidar observations were complemented by Aerosol Robotic Network handheld Sun photometer measurements, which revealed a mean total atmospheric column aerosol optical thickness of 0.05 for pure marine conditions (in the absence of lofted aerosol layers) and roughly 0.9 during a strong Saharan dust outbreak. The achieved data set was compared with first Consortium for Small Scale Modeling-Multi-Scale Chemistry Aerosol Transport simulations. The simulated vertical aerosol distribution showed good agreement with the lidar observations.

## 1. Introduction

As a consequent next step after the SAMUM (Saharan Mineral Dust Experiment) field campaigns [Heintzenberg, 2009; Ansmann et al., 2011] which took place close to the Saharan dust source (SAMUM-1, southern Morocco, 2006) and in the near range (SAMUM-2, Cape Verde, 2008) of the long-range transport regime of Saharan dust, we conducted multiwavelength Raman and polarization lidar observations aboard the research vessel (R/V) *Meteor* to characterize the Saharan Air Layer along the main transport route from western Africa to the Caribbean [Prospero and Carlson, 1972] in April–May 2013. The main goal was a detailed height-resolved characterization of the optical properties of dust and mixtures of dust, biomass-burning smoke, and marine particles, as well as the changes in the optical properties of the aerosol layers during the long-range transport over 5000–8000 km distance from the main dust sources.

Such observations of aged, partly cloud-processed dust are required to better consider mineral dust changes during long-range transport as well as removal processes in atmospheric transport and climate models. Mineral dust is one of the major aerosol components in the atmosphere [Textor et al., 2006] and the tropical Atlantic provides almost ideal conditions to investigate dust and changes in the dust properties under almost undisturbed conditions far away from many anthropogenic aerosol sources in the Northern Hemisphere.

Recent spaceborne lidar observations have provided breakthrough height-resolved information of the vertical extent of dust outbreaks and seasonal shifts of the Saharan Air Layer over the Atlantic [Liu et al., 2008; Adams et al., 2012]. However, spaceborne lidar lack of resolution for detailed investigations of processes. Aerosol property retrievals might be also biased by adjacent clouds and/or necessary assumptions [e. g., Tackett and Di Girolamo, 2009; Tesche et al., 2013].

In this analysis we will present first results of an approach to characterize pure and mixed Saharan desert dust during its transatlantic advection to the Caribbean by advanced lidar measurements. We deployed a Polly<sup>XT</sup> aboard the R/V *Meteor* and conducted continuous observations during a cruise from the Caribbean (16°N, 61°W) to the west coast of Africa (17°N, 25°W) in April–May 2013. In this way, the optical properties of 2–3 to >10 days old Saharan dust could be determined. In addition, the entire data set offers the opportunity to validate aerosol transport model simulations of the vertical dust distribution over the Atlantic. Within this work, we used the regional modeling system COSMO-MUSCAT (Consortium for Small

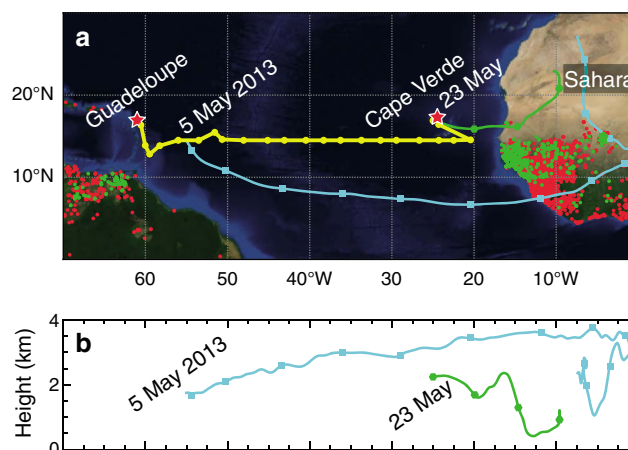


**Figure 1.** (a) Map of the cruise with R/V *Meteor* from Guadeloupe to Cape Verde from 29 April to 23 May 2013 (yellow line). Hybrid Single-Particle Lagrangian Integrated Trajectory (HYSPPLIT) backward trajectories (cyan and green lines) indicate the transport path of observed dust layers on 5 and 23 May 2013. Symbols at the trajectories (00:00 UTC) indicate the residence time in days. Active fires for 20 to 30 April 2013 (red dots) and from 17 to 22 May 2013 (green dots) are shown. (b) From HYSPPLIT calculated heights at which the African aerosol was transported before the observation above R/V *Meteor*.

Scale Modeling-Multi-Scale Chemistry Aerosol Transport model) for a first attempt to simulate the vertical distribution of Saharan dust. The COSMO-MUSCAT simulations also offered a well-suited source identification of the observed free-tropospheric aerosol layers in addition to standard backward trajectory analyses.

The paper is organized as follows. In section 2 a brief overview about the cruise track, the used measurement instruments, and the model are listed. Afterward, we present the observed and simulated aerosol conditions along the cruise. In addition, an in-depth lidar data analysis of two case studies is presented in section 3. Finally, we conclude our findings.

## 2. Experiment

Multiwavelength Raman and depolarization lidar data measurements were conducted during the transatlantic cruise M96 of the R/V *Meteor* from Guadeloupe (16°N, 61°W) to Cape Verde (17°N, 25°W), respectively from 29 April to 23 May 2013. Figure 1 shows the cruise track of R/V *Meteor* (yellow line) across the Atlantic Ocean over a distance of  $\approx 4000$  km. For this purpose the current most advanced version of the so-called Polly<sup>XT</sup> lidars [Engelmann *et al.*, 2012] was operated as part of the OCEANET-Atmosphere platform aboard R/V *Meteor*. The aim of OCEANET-Atmosphere is to investigate the aerosol and cloud effect [Kanitz *et al.*, 2013] on the Earth's radiative budget over the ocean and includes lidar, Sun photometer, microwave radiometer, pyranometer, pyrgeometer, and the measurement of standard meteorological parameter. Routinely launched radiosondes complement the atmospheric shipborne observations.

The operation of Polly<sup>XT</sup> allows for the determination of vertical profiles of the particle backscatter and extinction coefficient at 355, 532, and 1064 nm, and 355 and 532 nm, respectively. In doing so, aerosol layers can be characterized in terms of the size-dependent Ångström exponent and the lidar ratio, which depends on the shape and the chemical composition of the particles as well [Ansmann and Müller, 2005]. Polly<sup>XT</sup> is equipped with polarization sensitive channels at 355 and 532 nm, which serves as another information of the particle shape [Freudenthaler *et al.*, 2009]. An additional near-range receiver unit enables the determination of the particle backscatter and extinction coefficient down to 120 m above ground level under favorable conditions.

Accompanying observations include handheld Sun photometer measurements in the framework of the Maritime Aerosol Network from the Aerosol Robotic Network (AERONET) [Smirnov *et al.*, 2009].

The obtained profiles of the vertical distribution of the Saharan dust layer were simulated with COSMO-MUSCAT. The regional dust model was developed during the SAMUM campaign and is explained in

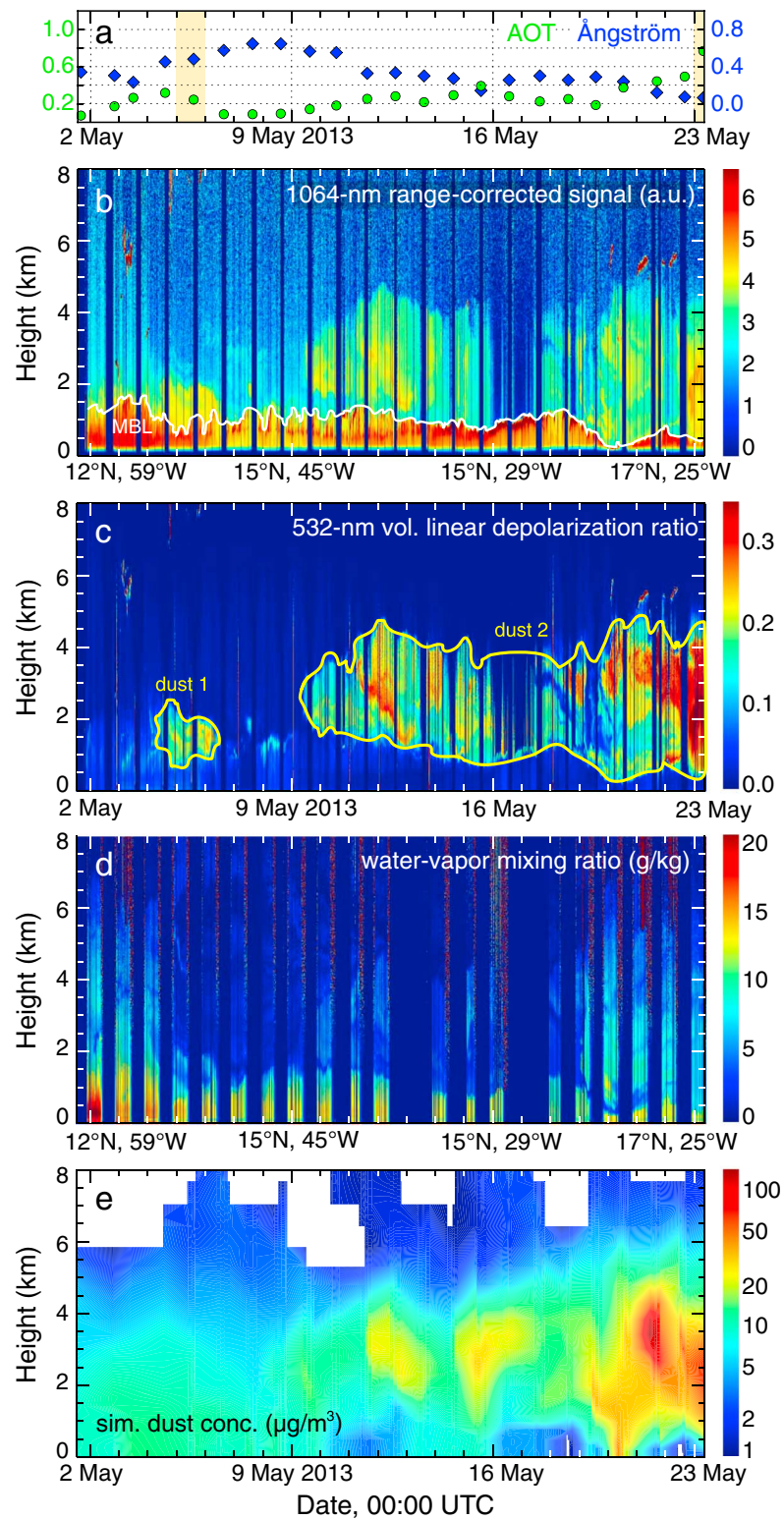


**Figure 2.** (a) Daily mean aerosol optical thickness at 500 nm (AOT, green circles) and Ångström exponents (440/870) as determined with Sun photometer aboard R/V *Meteor* from 60°W to 20°W in May 2013. Orange-shaded sections highlight the measurement days of the in-depth analysis. Height-time display of lidar measurements during the cruise in terms of the (b) 1064 nm range-corrected backscatter signal, (c) the 532 nm volume linear depolarization ratio, and (d) the water vapor mixing ratio. A white line in Figure 2b indicates the marine boundary layer (MBL) height. Yellow lines in Figure 2c highlight the main part of the lofted aerosol layers which contain considerable amounts of nonspherical dust. (e) COSMO-MUSCAT simulation results of the vertical distribution of dust concentration in  $\mu\text{g m}^{-3}$ .

detail by *Heinold et al.* [2007]. The dust emission, transport, and deposition of five independent aerosol size classes between 0.1 and 25  $\mu\text{m}$  radius are modeled with MUSCAT based on the meteorological information of COSMO. The vertical grid has 40 layers from the surface to the tropopause with a first-layer depth of about 68 m [*Heinold et al.*, 2011; *Tegen et al.*, 2013]. The final simulation results offer a suitable tool for a detailed dust source apportionment.

### 3. Observations

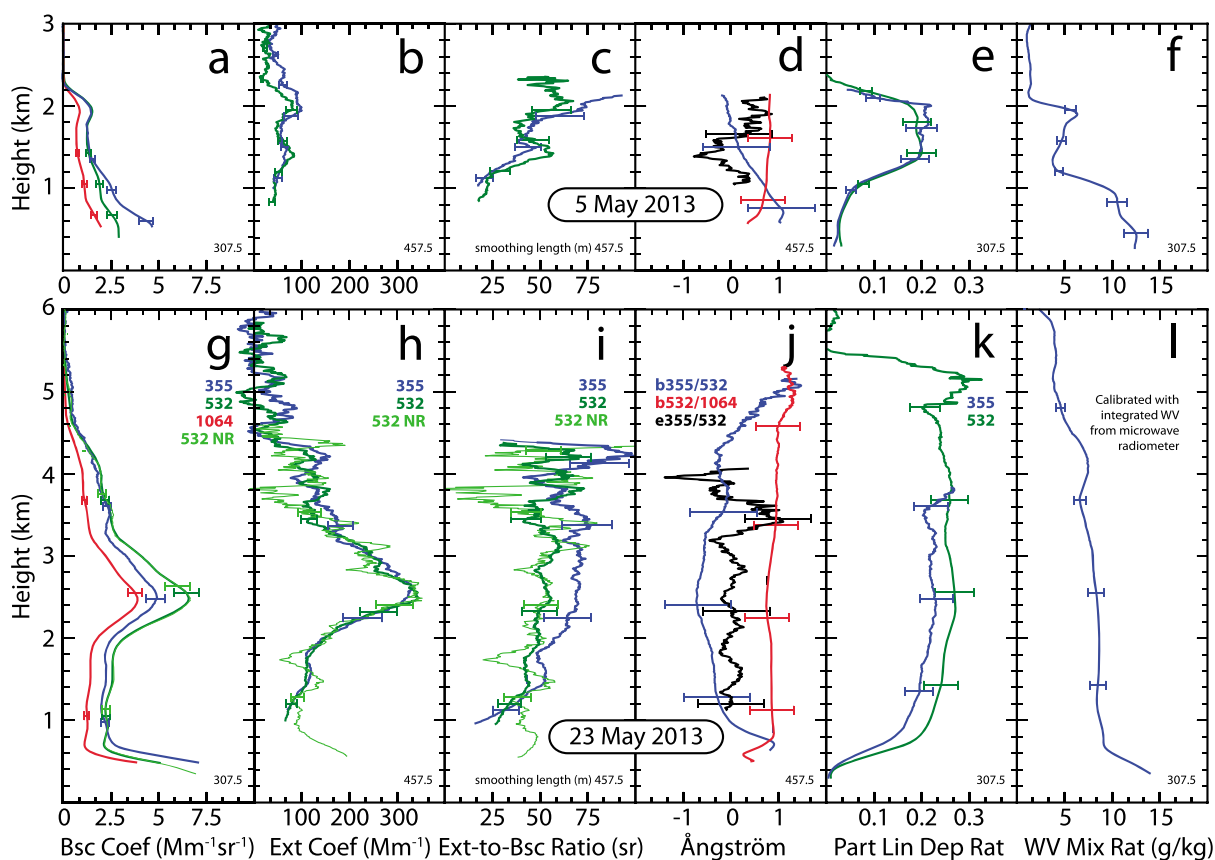
From 29 April to 23 May 2013 aerosol observations with lidar and Sun photometer were performed aboard the R/V *Meteor* to determine Saharan dust properties in dependence of its atmospheric residence time. During the cruise daily mean aerosol optical thickness (AOT in Figure 2a, green filled circles) varied between 0.09 on 7 May (almost pure marine conditions) [*Smirnov et al.*, 2009; *Kanitz et al.*, 2013] and 0.8 at 500 nm on 23 May 2013, respectively. The Ångström exponent from Sun photometer measurements for 440 and 870 nm wavelength (Figure 2a, blue diamonds and green filled circles) was almost zero when the AOT was highest and clearly indicated the presence of large dust particles. Figure 2b presents a composite of all shipborne lidar measurements of the cruise in terms of the 1064 nm range-corrected backscatter signal. Blue vertical lines result from measurement interruptions due to high Sun elevation around 1200 local time. Red and orange colors in the lower most 2 km indicate the marine boundary layer (MBL). The MBL height varied between 300 and 1700 m height. From 45°W to the Cape Verde region lofted dust was observed up to 5 km height (Figure 2, green and yellow colors). The volume linear depolarization ratio at 532 nm shown in Figure 2c clearly indicates the dominance of Saharan dust (nonspherical scatterer) in these layers (Figure 2, yellow to red colors). Figure 2c shows also an aged dust layer in the area around 55°W observed from 4 to 6 May 2013. This plume reached to 2.5 km height only and was observed after a travel time of 12 days (7500 km) as indicated by Figure 1 (cyan squares).

Figure 2d shows the height-time display of the determined water vapor mixing ratio (WV). The highest WV was found in the MBL up to  $\approx 20 \text{ g kg}^{-1}$ . In the dust layers WV ranges mostly around 4–5  $\text{g kg}^{-1}$ , despite the period from 19 to 23 May 2013. In accordance, radiosonde launches showed 30–80% relative humidity in the dust layers. The WV observations with lidar (Figure 2d) show complex patterns in the vertical and horizontal WV distribution along the cruise that will be discussed elsewhere.

COSMO-MUSCAT simulations were performed to estimate the atmospheric dust concentration as shown in Figure 2e. The simulated vertical dust distribution is in good agreement with the lidar observations (cf. Figures 2b and 2e). Especially, patterns in the height-time display showing high volume depolarization ratios (Figure 2c) from 11 to 13 May and 21 to 23 May are well reproduced from the simulations. The derived dust concentration varies between 10 and 20  $\mu\text{g m}^{-3}$  in the first observed dust layer (4–6 May 2013) and from 10 to 150  $\mu\text{g m}^{-3}$  in the second observed dust layer (10–23 May 2013).

HYSPLIT backward trajectories [*Draxler and Rolph*, 2003] were calculated for the observed dust layer from 4 to 6 May 2013. An example is presented in Figure 1 (cyan line). In agreement to the COSMO-MUSCAT simulations, the dust uptake occurred in the area of Mauritania and Mali >10 days (a travel distance of around 7500 km) before the observation when the air masses were close to the ground (Figure 1b). Within this period (20–30 April 2013) a considerable amount of active fires was determined in the Saharan dust outflow with the Moderate Resolution Imaging Spectroradiometer (MODIS) [*Giglio et al.*, 2006] as shown by red dots in Figure 1a, which has to be taken into account in the data analysis.

The dust optical properties derived from the lidar measurement on 5 May 2013, 22:00–23:35 UTC are shown in Figure 3 (top). The main layer extended from 1.2 to 2.0 km and was well mixed as the height-constant value of the particle linear depolarization ratio ( $\delta_p$ ) in this layer indicates (Figure 3e). The  $\delta_p$  values in this height range were roughly equal and about 20% at both wavelengths of 355 and 532 nm. Figure 3d shows mean extinction and backscatter-related Ångström exponents of  $0.1 \pm 0.4$  and  $0.1 \pm 0.2$  (355/532 nm) for this layer, respectively. The backscatter-related Ångström exponent for 532/1064 nm wavelength is  $0.8 \pm 0.0$ . The mean lidar ratio  $S_p$  is  $45 \pm 12$  and  $45 \pm 7$  sr at 355 and 532 nm (Figure 3c). The AOT of the lofted layer in the observed height range was about 0.05. The increased  $\delta_p$  and the wavelength-independent backscatter and extinction coefficients at 355 and 532 nm indicate dust [*Kanitz et al.*, 2013]. However, the observed lidar ratio and  $\delta_p$  are considerably lower than respective values for pure dust close to the Saharan dust source ( $S_p \approx 50\text{--}60$  sr,  $\delta_p \approx 30\text{--}35\%$ ) [*Freudenthaler et al.*, 2009; *Tesche et al.*, 2009]. These lower values



**Figure 3.** Averaged profiles of the (a) backscatter and (b) extinction coefficient, (c) extinction-to-backscatter ratio, (d) Ångström exponent, (e) particle linear depolarization ratio, and (f) water vapor mixing ratio as determined on 5 May 2013 22:00 to 23:25 UTC. (g–l) The same as in Figures 3a–3f but for 23 May 2013 00:05 to 03:25 UTC. NR denotes the near-range receiver unit. Profiles of backscatter coefficient, particle linear depolarization ratio, and water vapor mixing ratio are smoothed with 307.5 m, others with 427.5 m.

most likely result from the presence of hygroscopic fine-mode aerosol particles or marine aerosol. Also, the COSMO-MUSCAT simulations reveal a considerable mixture of aerosol types in the observed dust layer.

About 3700 km closer to the Saharan desert dust was observed until the end of the cruise on 23 May 2013. The atmospheric residence time of the second dust layer presented in Figure 2 was comparably short with roughly 2 days as indicated by backward trajectory analysis (Figure 1, green line). The simulations with COSMO-MUSCAT showed an intensive dust outbreak in the Aoukar region (south east Mauritania), which increased the AOT of the overall Saharan dust outflow from about 0.3 to 1.0. Active fires (Figure 1, green dots) occurred mostly in the south of the transport path during the time period from 17 to 22 May 2013 (Figure 1).

The optical properties of this second case (23 May, 00:00 to 01:30 UTC) are shown in Figure 3 (bottom). The layer extended from 0.7 to 4.8 km height with maximum extinction coefficients of  $340 \text{ Mm}^{-1}$  (Figures 3g and 3h). The dust-related AOT at 532 nm was approximately 0.6. For the central part of the dust plume (1.5–3.5 km height) we found mean values for the lidar ratio of  $64 \pm 8$  (for 355 nm) and  $50 \pm 5$  sr (for 532 nm). Mean extinction and backscatter-related Ångström exponents are  $0.1 \pm 0.3$  and  $-0.5 \pm 0.1$  at 355 and 532 nm wavelength, respectively (Figures 3i and 3j). The mean backscatter-related Ångström exponent computed from the values at 532 and 1064 nm is  $0.8 \pm 0.1$ . The mean  $\delta_p$  is  $22 \pm 1$  and  $26 \pm 1\%$  at 355 and 532 nm, respectively. These mean values are in reasonable agreement with the findings of the summer campaign of SAMUM-2 at Cape Verde from 24 May to 17 June 2008. During SAMUM-2 pure dust layers were observed from 0.7 to 6 km height. Lidar ratio values were about 53–54 sr ( $\pm 10$ ) at both wavelengths, and  $\delta_p$  values of  $31 \pm 10\%$  at 532 nm were observed [Tesche *et al.*, 2011]. The higher 355 nm lidar ratio observed on 23 May 2013 may however indicate the presence of some smoke on this day. This hypothesis is corroborated by the relatively small  $\delta_p$  values of around 26% at 532 nm.

Figure 3g shows an unusual wavelength dependence of the backscatter coefficient, i.e., a smaller backscatter coefficient at 355 than at 532 nm in the height range from 1 to 3 km height. This behavior was found in all dust layers from 18 to 23 May 2013. *Balis et al.* [2004] reported the same feature for a series of Saharan dust observations at Thessaloniki, Greece. Backscatter-related Ångström exponent of  $-0.9$  were presented by *Murayama and Sekiguchi* [2006] for an Asian dust layer. In a simulation study, T-Matrix code calculations of spheroids and a lognormal particle size distribution from 0.5 to 4.1  $\mu\text{m}$  reproduced this wavelength dependence [Murayama and Sekiguchi, 2006], without a wavelength-dependent complex refractive index. If this simulation approach is suitable for dust emissions from the Aoukar region needs to be further analyzed under consideration of a larger range for the dust particle size distribution, dust mixtures, and irregularly shaped dust particles [Gasteiger et al., 2011].

It becomes increasingly obvious that smoke has to be considered to always be part in dust plumes during the whole burning season. This finding can not be clearly obtained from traditional measurements (e.g., Sun photometer, Ångström exponent  $\approx 0.1$ ), but from lidar backscatter, lidar ratio, and  $\delta_p$ .

#### 4. Summary

Recent shipborne lidar measurements across the tropical Atlantic along the main route of Saharan dust long-range transport toward America were used to show the optical properties of almost fresh and aged dust layers. Significant differences in the dust optical properties in the discussed two dust plumes were found and may result from aging effects. The reason for these changes with transport need to be analyzed in comprehensive data analysis on day-by-day basis. First COSMO-MUSCAT simulations of the measurements showed a good agreement in the temporal process of the vertical dust distribution. Within the simulations a maximal dust concentration of  $150 \mu\text{g m}^{-3}$  was calculated. The day-by-day lidar data analysis will be used for further model comparisons with COSMO-MUSCAT and others, which will offer the estimation of the aerosol radiative effect as well.

#### Acknowledgments

We thank the R/V Meteor team and German Weather Service (DWD) for their support during the cruise M96. In the framework of EARLINET the work of Volker Freudenthaler and Holger Linne strongly improved the setup of Polly<sup>XT</sup>. We also appreciate the effort of AERONET MAN to equip research vessels with Sun photometer for atmospheric research.

The Editor thanks two anonymous reviewers for their assistance in evaluating this paper.

#### References

- Adams, A. M., J. M. Prospero, and C. Zhang (2012), CALIPSO-derived three-dimensional structure of aerosol over the Atlantic Basin and adjacent continents, *J. Clim.*, *25*, 6862–6879, doi:10.1175/JCLI-D-11-00672.1.
- Ansmann, A., and D. Müller (2005), Lidar and atmospheric aerosol particles, in *Lidar: Range-Resolved Optical Remote Sensing of the Atmosphere*, edited by C. Weitkamp, pp. 105–138, Springer, Singapore.
- Ansmann, A., A. Petzold, K. Kandler, I. Tegen, M. Wendisch, D. Müller, B. Weinzierl, T. Müller, and J. Heintzenberg (2011), Saharan mineral dust experiments SAMUM-1 and SAMUM-2: What have we learned?, *Tellus Ser. B*, *63*, 403–429, doi:10.1111/j.1600-0889.2011.00555.x.
- Balis, D. S., V. Amiridis, S. Nickovic, A. Papayannis, and C. Zerefos (2004), Optical properties of Saharan dust layers as detected by a Raman lidar at Thessaloniki, *Geophys. Res. Lett.*, *31*, L13104, doi:10.1029/2004GL019881.
- Draxler, R. R., and G. D. Rolph (2003), HYSPLIT (Hybrid Single-Particle Lagrangian Integrated Trajectory) Model, NOAA Air Resources Laboratory, Silver Spring, Md. [Available at <http://www.arl.noaa.gov/ready/hysplit4.html>.]
- Engelmann, R., D. Althausen, B. Heese, H. Baars, and M. Komppula (2012), Recent upgrades of the multiwavelength polarization Raman lidar Polly<sup>XT</sup>, *Proceedings of the 26th International Laser Radar Conference (ILRC)*, Porto Heli, Greece.
- Freudenthaler, V., et al. (2009), Depolarization ratio profiling at several wavelengths in pure Saharan dust during SAMUM 2009, *Tellus Ser. B*, *61*, 165–179, doi:10.1111/j.1600-0889.2008.00396.x.
- Gasteiger, J., M. Wiegner, S. Groß, V. Freudenthaler, C. Toledano, M. Tesche, and K. Kandler (2011), Modelling lidar-relevant optical properties of complex mineral dust aerosols, *Tellus Ser. B*, *63*, 725–741, doi:10.1111/j.1600-0889.2011.00559.x.
- Giglio, L., et al. (2006), Global estimation of burned area using MODIS active fire observations, *Atmos. Chem. Phys.*, *6*, 957–974, doi:10.5194/acp-6-957-2006.
- Heinold, B., et al. (2007), Regional modeling of Saharan dust events using LM-MUSCAT: Model description and case studies, *J. Geophys. Res.*, *112*, D11204, doi:10.1029/2006JD007443.
- Heinold, B., et al. (2011), Regional modelling of Saharan dust and biomass-burning smoke, *Tellus Ser. B*, *63*, 781–799, doi:10.1111/j.1600-0889.2011.00570.x.
- Heintzenberg, J. (2009), The SAMUM-1 experiment over southern Morocco: Overview and introduction, *Tellus Ser. B*, *61*, 2–11, doi:10.1111/j.1600-0889.2008.00403.x.
- Kanitz, T., A. Ansmann, R. Engelmann, and D. Althausen (2013), North-south cross sections of aerosol layering over the Atlantic Ocean from multiwavelength Raman/polarization lidar during Polarstern cruises, *J. Geophys. Res. Atmos.*, *118*, 2642–2655, doi:10.1002/jgrd.50273.
- Liu, Z., et al. (2008), CALIPSO lidar observations of the optical properties of Saharan dust: A case study of long-range transport, *J. Geophys. Res.*, *113*, D07207, doi:10.1029/2007JD008878.
- Murayama, T., and M. Sekiguchi (2006), Large wavelength dependence of the lidar ratio in Asian dust layers observed by dual-wavelength Raman lidar, *Proceedings of the 23th International Laser Radar Conference (ILRC)*, Nara, Japan.
- Prospero, J. M., and T. N. Carlson (1972), Vertical and areal distribution of Saharan dust over the western equatorial North Atlantic Ocean, *J. Geophys. Res.*, *77*, 5255–5265, doi:10.1029/JC077i027p05255.
- Smirnov, A., et al. (2009), Maritime aerosol network as a component of Aerosol Robotic Network, *J. Geophys. Res.*, *114*, D06204, doi:10.1029/2008JD011257.
- Tackett, J. L., and L. Di Girolamo (2009), Enhanced aerosol backscatter adjacent to tropical trade wind clouds revealed by satellite-based lidar, *Geophys. Res. Lett.*, *36*, L14804, doi:10.1029/2009GL039264.

- Tesche, M., A. Ansmann, D. Müller, D. Althausen, R. Engelmann, V. Freudenthaler, and S. Groß (2009), Vertically resolved separation of dust and smoke over Cape Verde using multiwavelength Raman and polarization lidars during Saharan Mineral Dust Experiment 2008, *J. Geophys. Res.*, *114*, D13202, doi:10.1029/2009JD011862.
- Tegen, I., K. Schepanski, and B. Heinold (2013), Comparing two years of Saharan dust source activation obtained by regional modelling and satellite observations, *Atmos. Chem. Phys.*, *13*, 2381–2390, doi:10.5194/acp-13-2381-2013.
- Tesche, M., S. Gross, A. Ansmann, D. Müller, D. Althausen, V. Freudenthaler, and M. Esselborn (2011), Profiling of Saharan dust and biomass-burning smoke with multiwavelength polarization Raman lidar at Cape Verde, *Tellus Ser. B*, *63*, 649–676, doi:10.1111/j.1600-0889.2011.00548.x.
- Tesche, M., U. Wandinger, A. Ansmann, D. Althausen, D. Müller, and A. H. Omar (2013), Ground-based validation of CALIPSO observations of dust and smoke in the Cape Verde region, *J. Geophys. Res. Atmos.*, *118*, 2889–2902, doi:10.1002/jgrd.50248.
- Textor, C., et al. (2006), Analysis and quantification of the diversities of aerosol life cycles within AeroCom, *Atmos. Chem. Phys.*, *6*, 1777–1813, doi:10.5194/acp-6-1777-2006.